JOURNAL OF MATERIALS SCIENCE 26 (1991) 4527–4533

Dynamic observation of fracture in particulate-filled epoxy resins reinforced with rubber

G. VEKINIS*, P. W. R. BEAUMONT
Department of Engineering, University of Cambridge, Cambridge CB2 1PZ, UK
G. PRITCHARD, R. WAINWRIGHT‡
School of Applied Chemistry, Kingston Polytechnic, Kingston upon Thames, Surrey KT1 2EE, UK

Crack propagation in epoxy resins filled with alumina trihydrate has been observed by dynamic *in situ* scanning electron microscopy. Double torsion specimens were fractured inside a scanning electron microscope (SEM) connected to a video recorder. Characteristic features of the crack propagation process were observed. The fracture mode was mainly intergranular at low crack velocities, (ca. 10 μm/s) with evidence of filler particle cracking (transgranular fracture) at higher velocities or after acid-washing the particles. Extensive shear yielding of the epoxy matrix occurred between closely spaced filler particles within the crack tip damage zone. Post-mortem static observations of the fracture surfaces were also carried out. The addition of rubber toughening agents modified the crack propagation process. In some cases the rubber was present as fine, evenly distributed particles while in others there were coarser precipitates and/or what appeared to be rubber-rich epoxy phases. Ligamentary bridges across crack faces in the crack wake necked to fracture at low crack velocities but failed by cavitation under rapid loading. Energy dissipation by local shear yielding of the matrix was still prominent. Vinyl terminated rubber addition induced especially widespread yielding. Out-of-SEM determinations of tensile and fracture parameters were consistent with dynamic SEM observations.

1. Introduction

Alumina trihydrate (ATH) is frequently added to thermosetting resins such as unsaturated polyesters and epoxy resins to increase the critical oxygen index and reduce smoke evolution in the event of a fire. Compositions containing as little as 20 parts of ATH per hundred of resin by weight (pphr) suffer from drastically reduced tensile strength and elongation at break. It was therefore decided to observe the crack propagation process in ATH filled epoxy resins directly, in order to determine the mechanism of weakening and to establish how the crack propagation characteristics could be modified by rubber-toughening agents.

It is known, however, that ATH increases the strain energy release rate (G_{Ic}, or toughness) of epoxy resins [1] and theories involving crack pinning [2] have been invoked to explain the increase in G_{Ic} observed with some kinds of particulate-filled resins. The reduction in tensile strength can be explained by the weakening effect of, for example, shear bonding or debonding. Neglecting the plasticity observed at the crack tip, the reduction in strength can also be envisaged in terms of Griffith-type flaws [3] consisting of clusters of irregular ATH particles. The SEM examination described here was expected to show whether the crack propagation is predominantly intergranular or transgranular, whether extensive particle debonding occurs, and how various types of dispersed nitrile rubber phases contribute to the toughening process. It was expected to provide evidence of shear yielding, which is not visible by static post-mortem SEM examination, and to facilitate the observation of interactions between cracks and phases.

2. Experimental procedure

2.1. Materials

The epoxy resin used was Shell Epikote 816, which is a conventional DGEBA (diglycidyl ether of bisphenol A) resin modified by the addition of a reactive diluent. It was cured with Epikure T, a mixture of primary and secondary aliphatic amines. Aluminium trihydroxide, i.e. alumina trihydrate (ATH) was supplied by BA Chemicals Ltd. The grade used in this work was FRF 20 and the composition was 50 pphr. An ATH particle is shown as-received in Fig. 1a.

The ATH was used:

(a) as-received;

(b) washed with 1:1 v/v sulphuric acid: water solution;

* *Present address*: Institute of Materials Science, "Demokritos" National Research Centre, 15310 Ag. Paraskevi, Athens, Greece.

‡ *Present address*: Alcan Chemicals Ltd, Chalfont Park, Gerrards Cross, Bucks SL9 0QB, UK.

0022–2461/91 $03.00 + .12

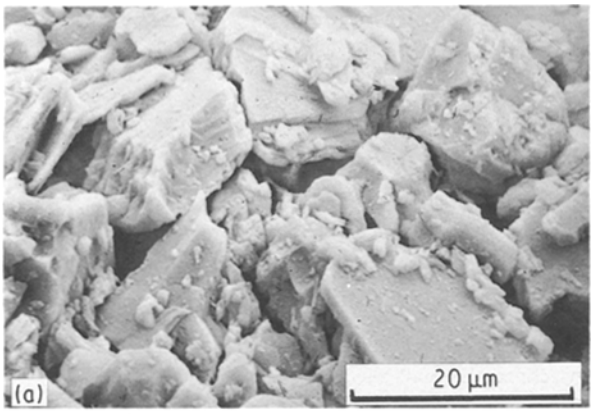

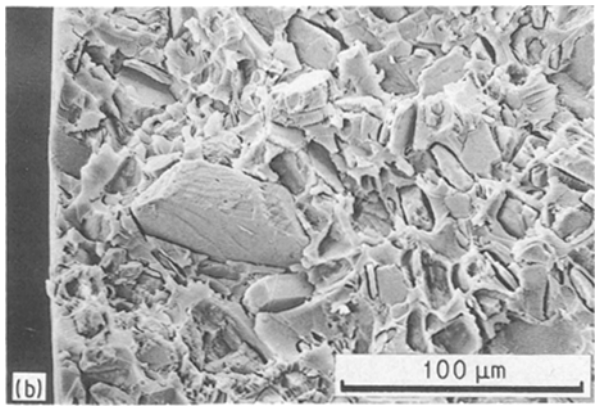

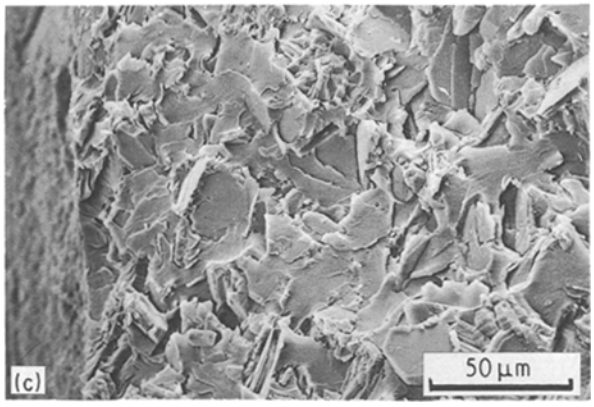

Figure 1 SEM observations of morphology of (a) as-received ATH particles, (b) specimen showing intergranular crack propagation with slow loading (10 μm min^{-1}) and (c) transgranular crack propagation with fast loading.

(c) surface treated with the coupling agent gamma aminopropyl triethoxy silane;

(d) surface treated with the release agent hexamethyl disilazane.

Three varieties of Hycar® butadiene-acrylonitrile copolymer toughening rubber were supplied by the B. F. Goodrich Co.:

(a) carboxyl terminated (CTBN);

(b) vinyl terminated (VTBN);

(c) amine terminated (ATBN).

2.2. Cure procedure

ATH powder was dispersed into the epoxy resin using a mechanical stirrer. The mixture was degassed under vacuum, followed by addition of the curing agent. After thorough mixing, the slurry was poured into a horizontal mould consisting of a glass base and a plasticine surround with a Melinex® sheet for mould release purposes. The mixture was degassed for a further 45 minutes and then cured at room temperature for 24 hours. The curing schedule was completed by post-curing at 80 °C for 3 hours.

10 pphr rubber was added to some compositions by dissolving 10 parts by weight of rubber in the resin at 50 °C before the addition of ATH.

2.3. Mechanical properties

Tensile strength, modulus and elongation to failure were determined from dumbell specimens machined from cast sheet, using a numerically controlled milling machine, and broken in an Instron tensile machine at 5 mm/minute. The G_{Ic} values were obtained using the tapered double cantilever beam (DCB) specimen. Critical stress intensity factors (K_{Ic}) (fracture toughness values) were determined using edge-notched rectangular tensile specimens.

2.4. Dynamic *in situ* loading jig

The materials were machined into double torsion specimens [4] measuring $50 \times 25 \times 1.5$ to 2 mm for loading in a special jig while the specimen was on the stage of the SEM. The surface to be observed was ground and polished using diamond paste to 1 μm diameter, and relief polished using a slurry of 0.05 μm aluminium oxide powder in water containing 1% potassium hydroxide. A 15 nm gold coating was applied by sputtering. The crack was introduced using a diamond-tipped circular saw, and sharpened with a new razor blade before loading.

The load application system was geared so that stable crack growth could be advanced at velocities of the order of 10 μm/minute. The groove depth was half the specimen thickness, and the loading points were 5 mm from the edge, to ensure uniform stress distribution at the notch tip. The distance between the top loading points was 20 mm, and between the bottom ones it was 5 mm. The jig was instrumented so that crack opening displacement, crack length, crack velocity, a stress–strain curve, crack tip stress intensity factor and other related parameters could be computed. In practice, however, the relative ductility of many of the samples meant that crack opening occurred by a mixture of mode I and mode II, and no such calculations were made.

2.5. SEM investigations

The SEM was a Cambridge Stereoscan 100 equipped with detectors for backscattered and secondary electrons, an X-ray analyser and an image store and enhancer. The ATH could be recognized as light-coloured angular particles in a darker epoxy resin matrix. The crack propagation characteristics of rubber-free epoxy resin and of ATH-filled epoxy resin

were first observed. Slow loading conditions were used for the dynamic SEM observations but the final fracture was carried out at more than 1 mm/minute, in order to compare the fracture characteristics under different strain rates. Slow crack propagation at 10 μm/minute favoured intergranular cracking (Fig. 1b) but fast loading produced many more transgranular cracks (Fig. 1c). All observations were recorded on videotape for subsequent analysis.

All specimens were finally fractured outside the SEM and both "slow" and "fast" fracture surfaces were examined subsequently inside the microscope.

3. Results and discussion

3.1. Mechanical properties

The mechanical properties of the materials are shown in Table I. The tensile properties follow the same trend previously reported by Radford [1] for ATH filled epoxy systems:

(a) addition of ATH to an epoxy resin increases the tensile modulus of the resulting particulate composite; and

(b) ATH significantly reduces the tensile strength and elongation at break.

An increase in tensile modulus is to be expected when a high modulus filler is dispersed in a relatively low modulus matrix.

Slight differences in tensile properties at constant volume fraction of ATH are probably due in part to the various surface treatments employed. For instance, acid treatment is likely to weaken the particles, essentially along their cleavage planes, as observed (see later) and to lead to low strength and elongation; conversely, untreated particles show a tendency to agglomerate, producing a similar but less pronounced effect. The addition of a rubber phase to filled samples increased the elongation but decreased the tensile strength and modulus.

ATH significantly increases the G_{Ic} values measured by the DCB method. The toughening of epoxy resins by relatively hard particulate fillers has many possible explanations. Evans *et al.* [5] have modelled the toughness enhancement of a glass bead/epoxy system, and suggested debonding and microcracking with dilatation plasticity as mechanisms. Toughening has sometimes been attributed to crack pinning [2], a process whereby a crack front is momentarily arrested by an array of ATH particles. The crack bows out between neighbouring particles before finally breaking away, dissipating energy in the process. However, although crack pinning probably occurs with other particulate fillers, e.g. glass beads [6], it is unlikely to take place with the very weak ATH particles. The increase in toughness is probably due to crack tip blunting and extensive shear yielding at stress concentrations; both processes are visible under dynamic SEM examination.

The fracture toughness, K_{Ic}, is further increased by a dispersed rubber phase. This effect has been shown previously [7] to be due to energy dissipating mechanisms initiated by the rubber dispersion. Mechanisms such as rubber cavitation [7, 8], tearing, plastic shear yielding [9] and rubber tearing [10] have been reported.

Two kinds of fracture behaviour were observed during the fracture toughness testing of the samples, the results of which are shown in Table I:

(a) crack initiation followed by crack arrest, i.e. stick-slip cracking; and

(b) slow, stable ductile crack growth.

The crack behaviour observed both in the dynamic SEM studies and in DCB fracture toughness tests depended on the presence or absence of ATH and on the loading rate. Stick-slip crack growth occurred mostly in the unfilled materials, whilst slow stable growth was dominant in the filled materials. Similar observations were made by Beaumont and Young [11] in quartz-filled epoxy resins. On increasing the loading rate, stick-slip behaviour became more apparent in the filled materials as well. Static SEM observations of filled samples fractured at low and high loading rates indicated that the fracture surfaces created in stick-slip crack opening were smooth (transgranular failure) in comparison with those formed in slow stable growth (intergranular failure).

For ATH-filled, rubber-free samples, the highest fracture toughness was obtained with silane treated ATH, and the lowest values with the acid treated samples.

TABLE I Mechanical properties of ATH-filled, rubber toughened epoxy resins

ATH (pphr)	ST	Rubber	Tensile modulus (GPa)	Tensile strength (MPa)	Elongation at break (%)	G_{Ic} (kJ m^{-2})	K_{Ic} (MN m$^{-3/2}$)
0	–	–	3.23	82	4.9	0.07	0.4
0	–	ATBN	2.1	56	3.7	0.74	2.2
50	–	–	4.4	54	1.6	0.29	1.4
50	–	ATBN	3.3	40	1.8	0.57	1.3
50	RA	–	4.9	62	1.7	0.33	1.3
50	silane	–	4.6	62	1.7	0.36	1.4
50	acid	–	5.2	35	0.7	0.21	0.8
0	–	CTBN	2.1	49	3.5	0.99	2.4
50	–	CTBN	3.2	28	1.6	0.64	1.5
0	–	VTBN	22.2	54	2.5	0.84	2.2
50	–	VTBN	3.0	25	1.4	0.65	1.5

ST = ATH surface treatment.
RA = release agent.

3.2. General observations: unfilled epoxy samples

The gold coating obscured any underlying yielding or microcracking of the matrix, because it was insufficiently ductile to mimic the substrate behaviour and so it underwent extensive microcracking. This is clearly visible during dynamic SEM examination. Samples loaded outside the SEM without a gold coating, and subsequently examined inside the SEM, showed localised shear yielding of the same areas where the gold was observed to microcrack during *in situ* observations.

All specimens displayed a plastic yield zone of between 0.5 and 2 mm. Unfilled epoxy samples were flexible, and the loading jig could not accommodate a large crack extension. These "pure" epoxy samples showed a small plastic zone at the crack tip, in which a number of secondary microcracks were observed to initiate and propagate. The secondary cracks arrested at the same time as the main crack, which later re-initiated at a point behind the original crack tip. Shear yielding was extensive, and small epoxy ligaments were observed to bridge the fracture surfaces in the crack wake, finally fracturing after a short extension. Slow crack growth was accompanied by crack arrest and crack tip blunting. In contrast, fast crack growth resulted in a smooth fracture surface appearance. Fig. 2 shows an ATBN rubber-epoxy precipitate within the epoxy matrix. Ligaments can be seen bridging the wake of the nearby crack.

No crazing was observed in the epoxy matrix. This is consistent with the belief that crazing requires a high level of ductility typically associated with highly stressed, uncrosslinked thermoplastics [12] such as polymethyl methacrylate (PMMA) and polystyrene. The addition of rubber does enhance ductility in epoxies and the stretching of ligaments (see below) was especially prevalent in rubber-rich epoxy regions. The observation that crazing does not occur in this epoxy resin under the conditions described does not exclude the possibility that it could occur in very thin sections of lightly crosslinked epoxy resins, since ductile–brittle transitions are thickness-dependent. Thus a transmission electron microscope section might display limited crazing [13–14].

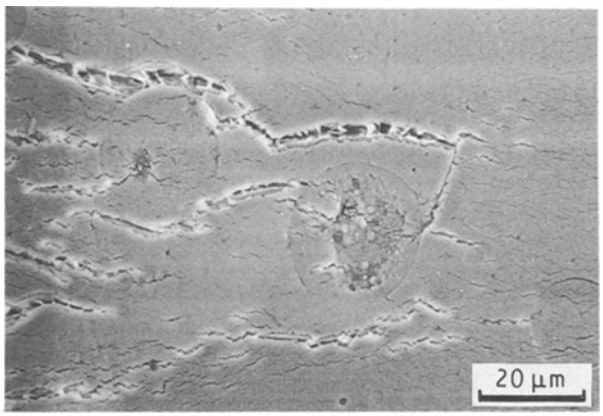

Figure 2 An ATBN rubber precipitate containing epoxy inclusions surrounded by the epoxy matrix. Ligaments can also be seen bridging the crack wake.

3.3. ATH surface treatment

The particles of untreated ATH were angular, but sulphuric acid treatment induced some rounding at the edges, as intended. Unfortunately, acid washing induced multiple cleavage cracks. The acid-washed particles embedded in epoxy resin also showed a very high incidence of cracks. These observations correlated with transgranular crack propagation through the filled resin specimens during loading, and with low composite tensile strength values (see Table I).

Silane treatment of the particles was carried out in a mechanical mixer, and the resulting particles were again less angular than the controls because of mechanical attrition. The particle size distribution had also shifted towards larger sizes, possibly because of a particle settling effect. The silane-treated samples showed the least transgranular cracking, i.e. less than the controls and much less than the acid-washed ATH samples. The silane-treated ATH filled samples also showed the most extensive microcracking of the gold surface coating, indicating a great deal of shear yielding, probably because of a limited capacity for energy absorption by debonding at ATH-epoxy interfaces. These factors imply toughness enhancement. The G_{Ic} value for silane treated ATH-epoxy materials was higher than that for any other ATH-epoxy mixture not containing rubber.

Treatment with hexamethyldisilazane release agent was expected to facilitate debonding of the ATH particles within the crack tip zone. In practice, it did not seem to produce any readily identified modification of the fracture process.

3.4. Crack propagation and ligamentation

As implied, cracks propagated sometimes through, and sometimes around the ATH particles; at low crack velocities intergranular fracture predominated, but faster cracks displayed a greater incidence of transgranular crack propagation. The experiments with samples loaded outside the SEM indicated that the shear yielding was localized around the crack tip, and mainly oriented normal to the applied stress.

Crack blunting and bifurcation occurred at low crack velocities, mainly in unfilled samples. Subsequent re-initiation often resulted in the formation of a few "bridges" or ligaments across the crack wake. At the same time, many smaller ligaments about the size of ATH particles formed between the crack faces

3.5. Rubber-toughened samples

3.5.1. Toughening

The rubber-toughened epoxy samples without ATH added always displayed higher G_{Ic} values than their untoughened analogues. Their tensile moduli were also slightly lower. Crack blunting was common, and shear yielding was frequently observed. This has been noted previously [15].

3.5.2. ATBN without ATH

ATBN contains very reactive functional amine groups which combine chemically with the epoxy groups in

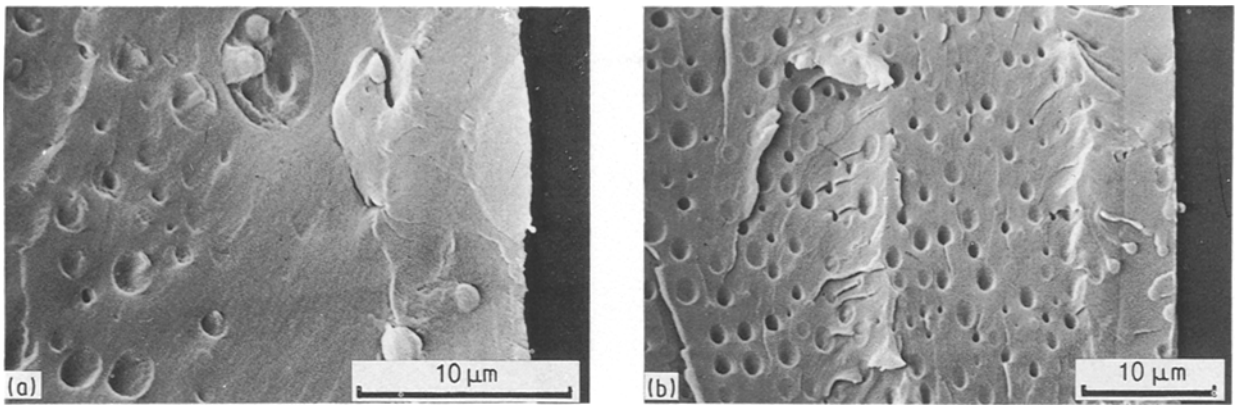

Figure 3 (a) Slow loading: the remains of rubber particles can be seen on crack faces; (b) Fast loading: cavitation occurs.

the resin. Carboxyl groups react more slowly. Thus the morphology of ATBN epoxy blends might be expected to differ from that of the other varieties. Distinctive, large spherical precipitates of diameter 10 to 20 μm were observed, which may have been solutions of ATBN in epoxy resin, or rubber particles containing epoxy occlusions. Such regions resemble those seen in ABS and some kinds of rubber-toughened polystyrene [16, 17]. Some much smaller ATBN precipitates were also present.

The crack tip plastic zone was extensive, and the microcracks in the gold coating extended over a large area in front of the crack tip. Observation of the crack propagation process showed that the rubber particles modified the process significantly. Extensive deformation near the notch tip preceded crack initiation, and arrest by blunting often followed almost immediately. At higher applied loads, propagation occurred by crack bifurcation, with re-initiation and the development of secondary microcracks. Rubber particles were seen bridging the crack, often stretching and necking before failing. It is possible to see the remains of rubber particles on the crack faces after slow loading (Fig. 3a) but no such remains could be observed at high loading rates where cavitation appears to be the predominant failure mode (Fig. 3b). This was especially apparent at high crack velocities.

3.5.3. ATBN with ATH

The large rubber-rich epoxy regions (Fig. 4) were more common than before, and they seemed to dominate the fracture process. There were also many very fine spherical particles of ATBN, typically 0.1 to 1.0 μm, which were probably too small to affect very much the crack propagation resistance, although they might have contributed to shear yielding.

Cracks usually passed through any large precipitates which did not debond from the surrounding matrix. These precipitates later stretched elastically to fracture in the crack wake. Other precipitates debonded from the matrix, and the cracks circumvented them.

The ATH fractured mainly by the intergranular mode, as the interface between ATH and matrix was also weak.

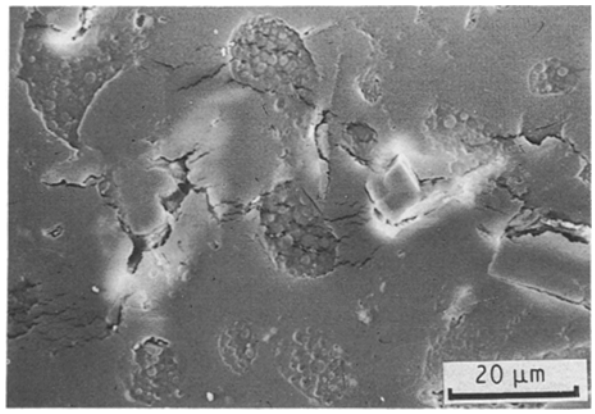

Figure 4 Several epoxy–rubber precipitates can be seen within the epoxy matrix in epoxy–ATBN–ATH compositions.

3.5.4. CTBN without ATH

Very fine (< 1 μm), well-distributed CTBN precipitates were found but with none of the larger rubber-epoxy regions of the kind seen in the ATBN toughened samples. The epoxy resin sometimes formed ligaments, which stretched considerably in the crack wake. No necking to fracture of CTBN precipitates was observed [15] but characteristic holes indicated cavitation.

3.5.5. CTBN with ATH

The CTBN precipitates were as described in the previous section. The ATH particles were frequently debonded from the surrounding matrix, with intergranular crack propagation, but a few suffered transgranular cracking, possibly along cleavage planes.

Two types of ligament were observed:

(i) isolated CTBN rubber particles; and (ii) plasticized, i.e. rubber-containing epoxy resin. Low loading rates resulted in mostly intergranular cracks with ligamentation and crack bridging; high loading rates produced more transgranular cracks and signs of cavitation. Many of the ligaments were observed to stretch (Fig. 5a), and to neck, rotate or tear, absorbing some of the fracture energy in the process. Sometimes the broken ligaments sprang back after failure, as would be expected for a rubber-rich material. The same ligament is shown in Fig. 5b immediately after

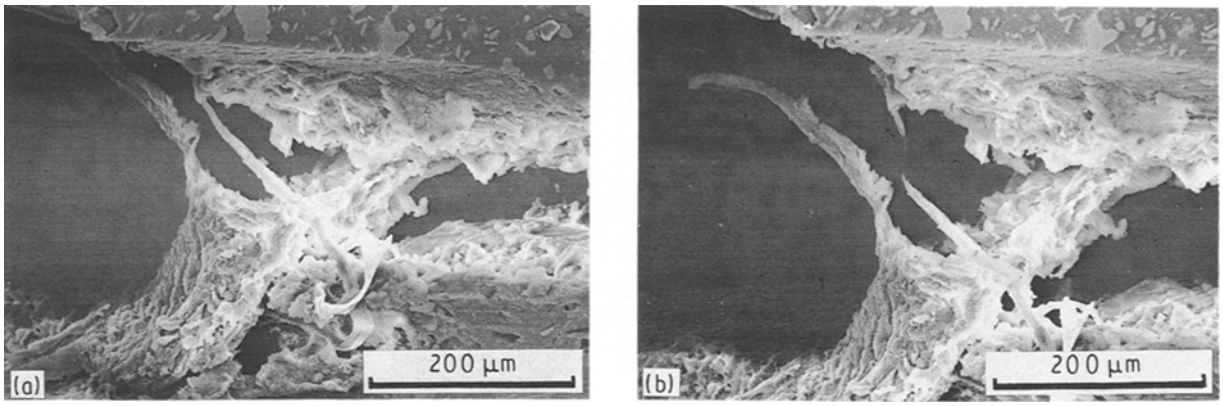

Figure 5 (a) A plasticized epoxy ligament in a CTBN-reinforced, ATH-filled specimen stretching to failure. The ligament extensibility is believed to be related to rubber content; (b) the same ligament after fracture.

fracture. The extent of stretching and elastic recovery may be related to the rubber concentration, but sufficiently thin ligaments of epoxy resin without rubber are capable of extensive plasticity in plane stress.

3.5.6. VTBN without ATH

Large (5 to 10 μm) VTBN precipitates were observed, without occlusions. The plastic zone was about 0.5 to 1 mm, judging from the extent of the gold microcracks. (The lower value corresponds with a calculated value of $K_{Ic} = 3\ MNm^{-3/2}$; compared with the experimental value for K_{Ic} of $2.2\ MNm^{-3/2}$). The cracks were surprisingly straight and not easily blunted or otherwise affected by the VTBN precipitates. The rubber particles failed by cavitation rather than necking, both at low and high loading rates. This was confirmed by examination of the failure process *in situ*. Ligamentary bridges were sometimes absent from cracks in VTBN-epoxy systems, as shown in Fig. 6. Shear yielding occurred over large areas, and not only near to the rubber precipitates.

3.5.7. VTBN with ATH

The VTBN precipitates were only 1 to 3 μm across. Again, two kinds of ligament bridged the cracks. Shear yielding was less noticeable, and the crack path was often irregular. Inter- and transgranular cracking took place both at low and high loading rates; the incidence of pre-existing cleavage microcracks probably controlled the extent of particle cracking.

4. Conclusions

1. Crack blunting and crack re-initiation could readily be seen with the double torsion specimens used inside the SEM.

2. A large shear yielding zone was always apparent at the crack tip.

3. Cracks propagated intergranularly around ATH particles at low loading rates, but transgranularly at high loading rates and especially in the presence of pre-existing cleavage plane cracks.

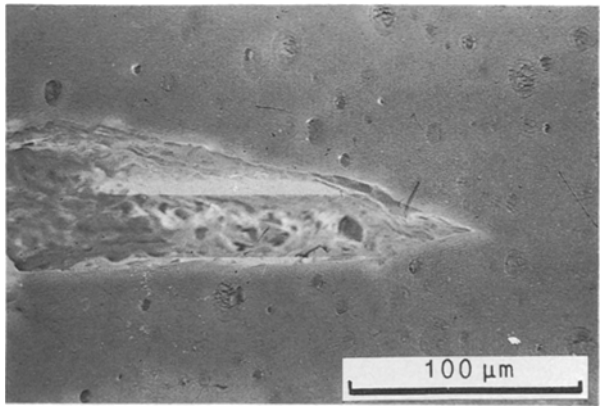

Figure 6 This particular crack in a VTBN unfilled epoxy sample shows no ligamentary bridges.

4. The rubber toughening agents generally increased the toughness of the material, partly by matrix plasticization and partly by the formation of rubber- and rubber-epoxy precipitates. The extent of toughness enhancement was believed to depend on the size of the dispersed rubber precipitates. The largest ones were associated with ATBN rubber because of its high reactivity. The dispersed particles sometimes failed by necking and sometimes underwent cavitation.

References

1. K. C. RADFORD, *J. Mater. Sci.* **6** (1971) 1286.
2. F. F. LANGE and K. C. RADFORD, *J. Mater. Sci.* **6** (1971) 1197.
3. A. J. KINLOCH and R. J. YOUNG, "Fracture Behaviour of Polymers" (Applied Science Publishers, London, 1983) p. 35.
4. B. J. PLETKA, E. R. FULLER Jr and B. G. KOEPKE, in "Fracture Mechanics Applied to Brittle Materials", ASTM STP 678, edited by S. W. Freiman (1979) 19.
5. A. G. EVANS, S. WILLIAMS and P. W. R. BEAUMONT, *J. Mater. Sci.* **20** (1985) 3668.
6. J. SPONOUDAKIS and R. J. YOUNG, *J. Mater. Sci.* **19** (1984) 487.
7. A. J. KINLOCH, S. J. SHAW, D. A. TOD and D. L. HUNSTON, *Polymer* **24** (1983) 1341.
8. A. M. DONALD and E. J. KRAMER, *J. Mater. Sci.* **17** (1982) 1765.
9. R. A. PEARSON and A. F. YEE, in "Tough Composite Materials", NASA Langley Research Center (Noyes Publications, Park Ridge, NJ07656 1985) pp. 157–177.

10. S. KUNZ-DOUGLASS, P. W. R. BEAUMONT and M. F. ASHBY, *J. Mater. Sci.* **15** (1980) 1109.
11. P. W. R. BEAUMONT and R. J. YOUNG, *J. Mater. Sci.* **10** (1975) 2334.
12. J. P. BERRY, in "Fracture VII", edited by H. Liebowitz (Academic Press, New York, 1972).
13. R. J. MORGAN, J. E. O'NEAL and D. B. MILLER, *J. Mater. Sci.* **14** (1979) 109.
14. R. J. MORGAN, in "Developments in Reinforced Plastics—1", edited by G. Pritchard (Applied Science Publishers, London, 1980) p. 222.
15. P. B. BOWDEN, in "The Physics of Glassy Polymers", edited by R. N. Haward (Applied Science Publishers, London, 1973).
16. S. NEWMAN and S. STRELLA, *J. Appl. Polym. Sci.* **9** (1965) 2297.
17. R. P. KAMBOUR and D. R. RUSSELL, *Polymer* **12** (1971) 237.

Received 18 July
and accepted 29 October 1990